Effects of Grading Shape on Liquefaction Focusing Pore Structures and Percolation

A. Kondo[(1)], E. Kohama[(2)]

[(1)] *Researcher, National Research and Development Agency National Institute of Maritime, Port and Aviation Technology, Port and Airport Research Institute, kondoh-a@pari.go.jp*

[(2)] *Head of Group, National Research and Development Agency National Institute of Maritime, Port and Aviation Technology, Port and Airport Research Institute, kohama-e83ab@pari.go.jp*

Abstract

When liquefaction occurs owing to seismic motion, erupted sand boils caused by increased excess pore water pressure are observed on the ground surface. Grain size analysis of these erupted sand points show very similar grain size distribution curves. In this study, we conducted model tests and numerical simulations to reveal this liquefaction mechanism considering the local permeability and pore structure. Based on the shaking table test using binary grading, it is confirmed that each maximum excess pore water pressure ratio shows agreement with its densest mixture content ratio, which content ratio also proportional to finer content ratio. This agreement for the liquefaction mechanism is evaluated by simulating the pore structure characteristics, such as void diameter and its continuity, using the discrete element method. The variation in the distribution of these indices shows good agreement with macroscopic permeability; it shows a proportional relation between the void size and its continuity. As for agreement with the experimental result, the pore structure indices show qualitatively good correspondence with excess pore water pressure rising content ratio. Based on the above quantitative agreements, the liquefaction potential according to various gradings is expressed by these interactions.

Keywords: Liquefaction; Grading Shape; Pore Structure

1. Introduction

When liquefaction occurs owing to seismic motion, erupted sand boils caused by increasing excess pore water pressure are observed on the ground surface. Grain size analysis of these erupted sand points has revealed similarities in the grain size distribution curves—grain sizes have been plotted from 0.1 to 0.3 mm. [1] Therefore, this similarity pointed to a finer content ratio as a representative factor for the evaluation of liquefaction potential in the Japanese technical standards for port and harbor facilities. This standard adopts two kinds of grading type boundaries based on the uniformity coefficient, and each grading type has two areas related to the liquefaction potential. [2, 3] After this grading screening, the liquefaction potential is categorized into four groups using the equivalent N value and equivalent bedrock acceleration. Regarding the relationship between this estimation method and the liquefaction mechanism, it is also well known that soil with the above-mentioned grain size show lower permeability. Lower permeability leads to impeding dissipation of pore water caused by deformation of soil. Therefore, excess pore water pressure rises till it exceeds the effective stress of the soil, resulting in liquefaction.

In this study, we examine the relationship between the liquefaction potential and permeability and grading shape from the viewpoint of pore structure. On the ground of this, excess porewater presure rising mechanism can be express by particle moving in deformation and pore structure changing as local permeability. In this paper, we only consider pore structure and attempt to evaluate it based on void size and its continuity. These two indexes definition are based on the thought of controlling construction size [4] and pore structures [5]. Consequently, we try to evaluate relationship between macroscopic and microscopic permeability through pore structure.

2. Liquefaction potential difference among various gradings

2.1 Model test specification

Fig. 1 shows a schematic diagram of the experimental apparatus and employed seismic wave. A sand specimen of length 365 mm, height 200 mm, and depth 160 mm is filled in a rigid tank. To observe the excess water pressure due to seismic motion, one water pressure gauge is installed in the vertical direction at 50 mm intervals from the horizontal center. These gauges are tied by a string so that they are not displaced by liquefaction. Regarding the soil sample condition, the relative density is set to 50%. The seismic wave is a sine wave of amplitude 200 gal and frequency 10 Hz. This wave acts two times at an interval of 10 s to examine the re-liquefaction behavior.

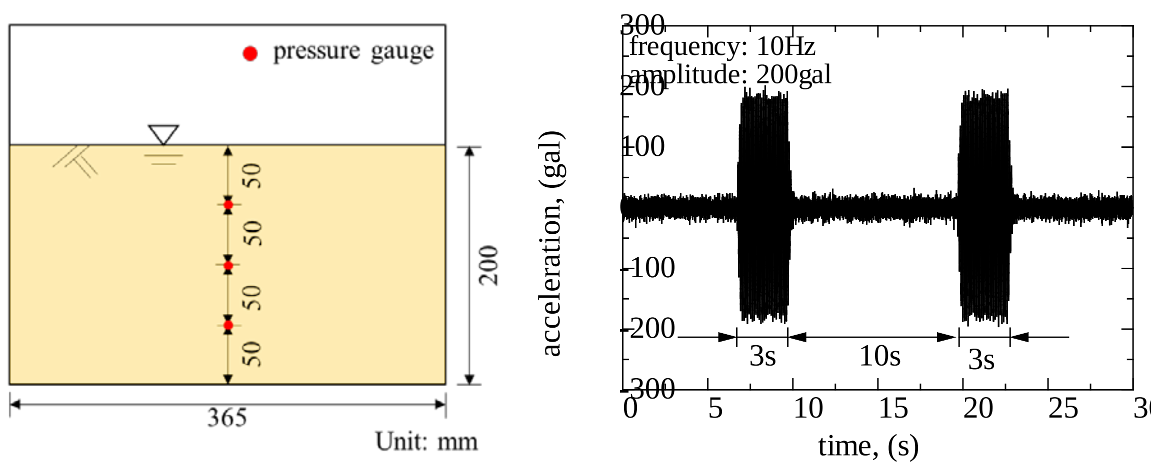

(a) Schematic illustration of experimental apparatus, (b) Adopted shaking waves

Fig. 1 – Model test specifications

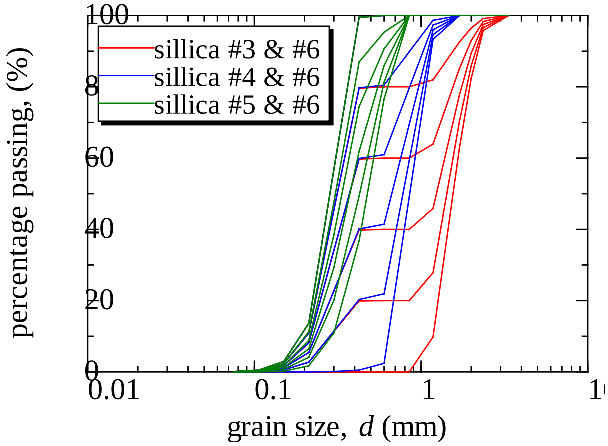

Fig. 2 – Grading shape,

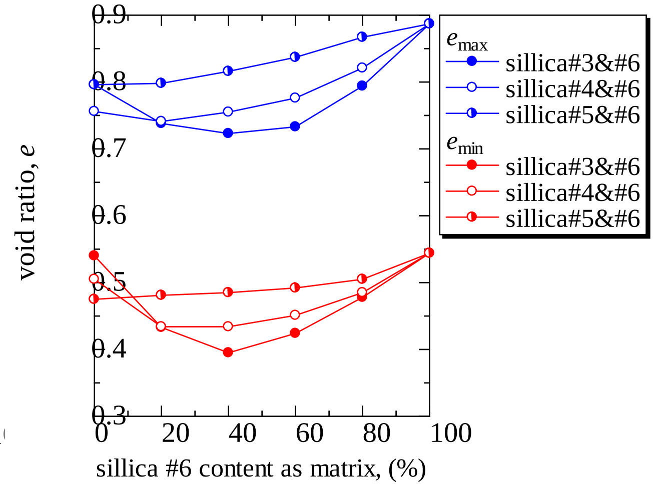

Fig. 3 – Void ratio against matrix content ratio

Table 1 – Specifications of adopted gradings

Mixture of sillica#3 - #6	Density, ρ_s	Max. grain size, D_{max}	Min. grain size, D_{min}	Median grain size, D_{50}	Uniformity coef., U_c	Curvature coef., U_c'	Permeability coef., k
Unit	g/cm^3	Mm	mm	Mm	-	-	cm/s
0% - 100%	2.64	3.35	0.075	0.285	1.64	1.01	4.48×10^{-2}
20% - 80%	2.64	3.35	0.075	0.306	1.69	0.95	6.20×10^{-2}
40% - 60%	2.64	3.35	0.075	0.351	1.86	0.88	7.18×10^{-2}
60% - 40%	2.64	3.35	0.075	1.14	5.73	0.36	8.57×10^{-2}
80% - 20%	2.64	3.35	0.075	1.36	5.44	3.05	1.83×10^{-1}
100% - 0%	2.64	3.35	0.850	1.48	1.40	0.98	1.17×10^{0}
Mixture of sillica#4 - #6	Density, ρ_s	Max. grain size, D_{max}	Min. grain size, D_{min}	Median grain size, D_{50}	Uniformity coef., U_c	Curvature coef., U_c'	Permeability coef., k
Unit	g/cm^3	Mm	mm	mm	-	-	cm/s
0% - 100%	2.64	1.70	0.075	0.285	1.64	1.01	4.48×10^{-2}
20% - 80%	2.64	1.70	0.075	0.317	1.72	0.92	6.22×10^{-2}
40% - 60%	2.64	1.70	0.075	0.371	1.97	0.87	6.06×10^{-2}
60% - 40%	2.64	1.70	0.075	0.665	3.24	0.68	7.69×10^{-2}
80% - 20%	2.64	1.70	0.075	0.779	3.02	1.73	1.84×10^{-1}
100% - 0%	2.64	1.70	0.212	0.853	1.45	0.93	3.79×10^{-1}
Mixture of sillica#5 - #6	Density, ρ_s	Max. grain size, D_{max}	Min. grain size, D_{min}	Median grain size, D_{50}	Uniformity coef., U_c	Curvature coef., U_c'	Permeability coef., k
Unit	g/cm^3	Mm	mm	mm	-	-	cm/s
0% - 100%	2.64	0.850	0.075	0.285	1.64	1.01	4.48×10^{-2}
20% - 80%	2.64	0.850	0.075	0.307	1.67	0.95	7.05×10^{-2}
40% - 60%	2.64	0.850	0.075	0.336	1.72	0.93	6.45×10^{-2}
60% - 40%	2.64	0.850	0.075	0.376	1.87	0.98	7.90×10^{-2}
80% - 20%	2.64	0.850	0.075	0.430	1.99	0.99	9.94×10^{-2}
100% - 0%	2.64	0.850	0.212	0.477	1.80	1.00	1.17×10^{-1}

Fig. 2 shows the adopted grading shapes, which consist of mixed standard silica sand called #3 to #6. Their content ratios are 0%, 20%, 40%, 60%, 80%, and 100%. Silica #6 is selected for matrix samples as a high liquefaction potential material. For simplicity, each case is expressed according to the following example: 80% of #3 and 20% of #6 case is expressed as #3-#6(80%-20%). Fig. 3 shows the maximum and minimum void ratios against the matrix content ratio of #6 which conducted by following the test method for minimum and maximum densities of sands (JIS A 1224:2009). Regarding the trend of the void ratio, some cases have the densest content ratio in the lower matrix sand mixture case, such as #3-#6(60%-40%) and #4-#6(60%-20%). This trend follows the Lade results. This means that the lower content ratio of the densest void ratio can be expressed as fine particles placed in the voids of coarse particles. Conversely, higher content ratio cases look like overfull voids—coarse particles floating in finer particles. In other words, it means that the densest content ratio can be thought as the switching boundary of the main structure as percolation. Table 1 shows specifications of the adopted grading, including density, maximum grain size, minimum grain size, median grain size, uniformity coefficient, curvature coefficient, and permeability coefficient. This permeability coefficient is also obtained by constant head permeability test following JIS A 1218:2009.

2.2 Model test specifications

Fig. 4 shows the representative time histories of the excess pore water pressure ratio of mixture cases #3 and #6. Fig. 4(a) shows case #3-#6(60%-40%) chosen as the switching point of the matrix content ratio, and Fig. 4(b) shows case #3-#6(80%-20%) with a lower matrix content ratio. Comparing these two time histories shows that only case (a) reaches liquefaction with an excess pore water pressure ratio of 1.0 at all depths during the first wave. During the second wave, case (a) shows a variation in the maximum pore water pressure ratio—liquefaction only occurs at a shallow depth of 5 cm. Case (b) also does not show a noticeable increase in the excess pore water pressure.

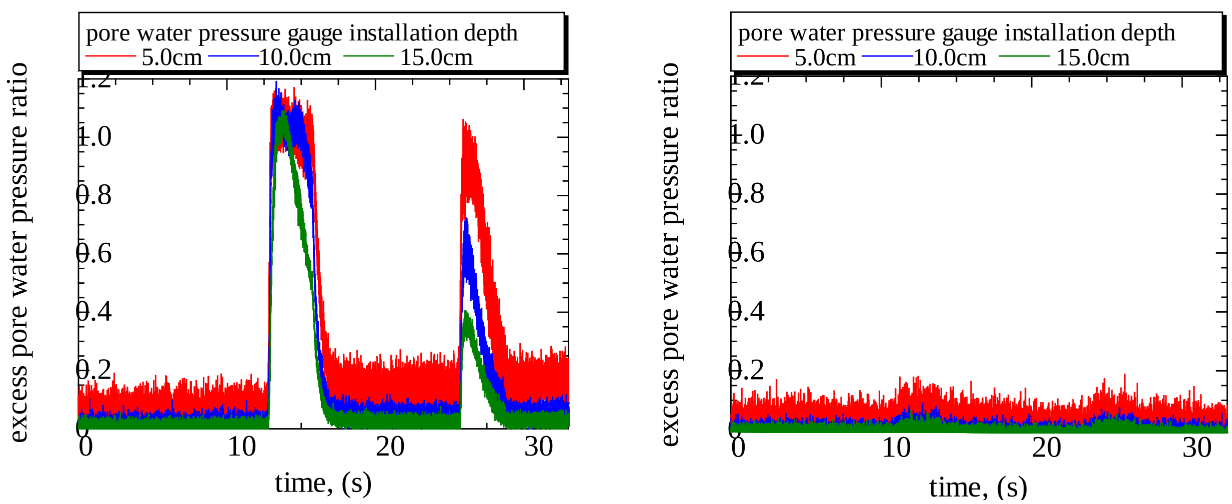

(a) Case #3-#6(60%-40%)

(b) Case #3-#6(80%-20%)

Fig. 4 – Representative time histories of excess pore water pressure ratio

Fig. 5 shows the relationship between the maximum excess pore water pressure ratio and the silica sand #6 content. Each grading case shows an increasing trend along with the matrix sample content. Moreover, its sharply increasing content ratio increases further with coarse grading size. The increasing matrix content ratio matches with the densest matrix content ratio. Therefore, it can be said that the matrix sand filling condition and void condition influence the liquefaction potential. Fig. 6 shows the relationship between the maximum excess pore water pressure ratio and permeability. According to the trend, a permeability of 0.2 cm/s can act as the boundary of liquefaction in this shaking condition. Moreover, compared with the variation in Fig. 5, it decreases.

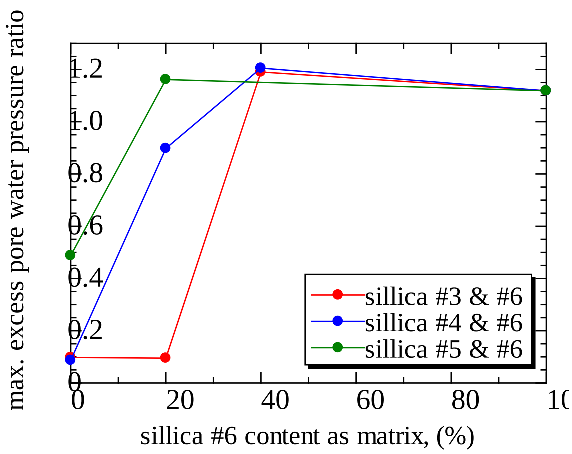

Fig. 5 – Maximum excess pore water pressure ratio at 10 cm depth during first wave

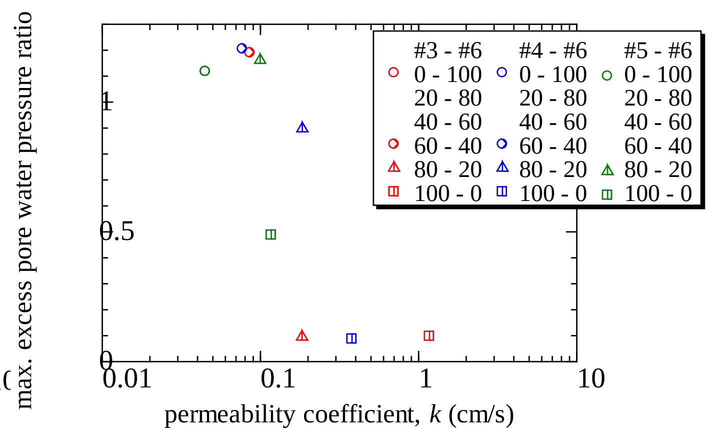

Fig. 6 – Boundary of permeability for increase in excess pore water pressure

3. Evaluation of pore structure in various grading shapes

3.1 Expression of permeability based on Hagen-Poiseuille flow

The previous section presented the experimental results for the liquefaction boundary against permeability. To confirm the correspondence, we try to find a relationship between permeability and grading shape in this section. As for the permeability estimation formula has proposed so far, such as Taylor and Creager formula. For thinking this estimation formula from viewpoint of pore structure, we picked up following Taylor's formula which expressed by multiplied representative grain size term and void ratio function term.

$$k = \frac{\gamma_w}{\eta} C_T {D_s}^2 \frac{e^3}{1+e} \tag{1}$$

where γ_w is the water density, η is the viscosity, C_T is a constant value, D_s is the representative grain size, and e is the void ratio. On this basis, the soil element can be expressed as a correction of tubes in a certain soil mass. In addition, a Hagen-Poiseuille flow can be thought of as a substitute for the internal flow of granular material. Moreover, as for the correspondence to each term, the representative grain size can be assumed to correspond with the hydraulic radius of the Hagen-Poiseuille channel; the void ratio function corresponds to the number of this flow channel.

Based on this thought, the permeability coefficient may be expressed in terms of the median grain size as the representative grain size. Fig. 7 shows this relation, but it cannot show good agreement.

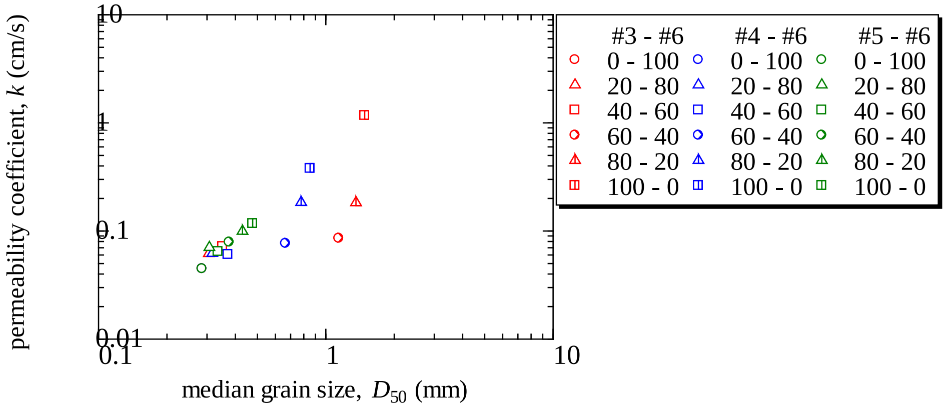

Fig. 7 – Expression of permeability coefficient in terms of the median grains size

3.2 Definition of pore structure

To more accurately express the permeability coefficient, we define pore structure on the basis of the Taylor formula; void size is the hydraulic radius of the Hagen-Poiseuille flow, and void continuity is its flow channel. Following this assumption, this section aims to describe the pore structure characteristics using sample packing by simulation with a three-dimensional discrete element method [7]. In addition, void size is defined as the assembly of the maximum sphere size in a certain void area, and its continuity is the movable distance of the minimum grain size particle.

Fig. 8 shows the determination procedure of void size and its continuity. First, grid points are set in discrete element packed samples, which sequence is 1/60 of minimum grain size. Then, the maximum void sphere size at that grid point is obtained. After that, in descending order, the void moves around till the largest void center is found. Hence, the pore void will be replaced by non-overlapping void spheres. Fig. 8(c) shows the judgment method between certain void D_n^{void} and next judgment target void D_{n+1}^{void}, which contact each other. If D_{n+1}^{void} is greater than D_n^{void}, D_n^{void} has continuity and void length plus D_{n+1}^{void}. But, if D_{n+1}^{void} is smaller than D_n^{void}, D_n^{void} changes to D_{n+1}^{void} because pore voids are narrowing. When D_n^{void} becomes lower than D_{min}, it means continuity reaches the end.

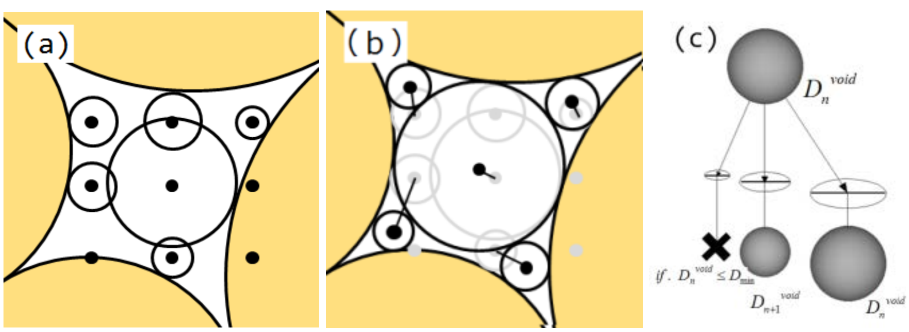

Fig. 8 – Determination procedure of void size and its continuity

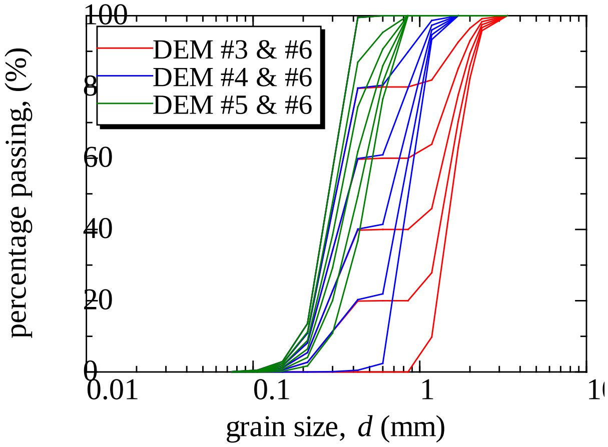

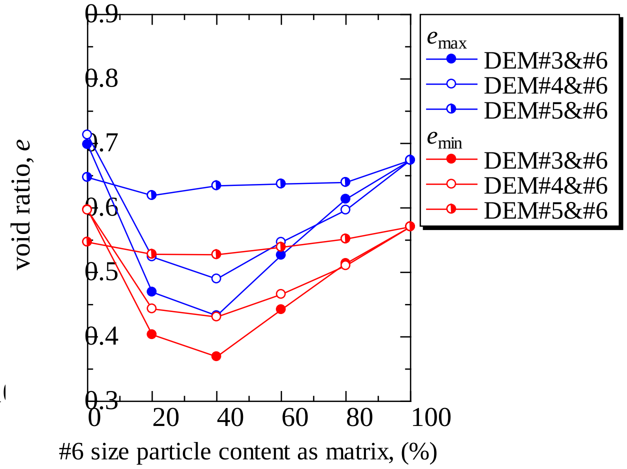

Fig. 9 – Grading shape in DEM simulation, Fig. 10 – Void ratio against matrix content ratio in DEM

Fig. 9 shows the grading shape adopted in this simulation, which is the same as that shown in Fig. 2. Fig. 10 shows the void ratio against the matrix content ratio in the discrete element method simulation, in which packing condition simulated by controlling six wall boundary moving. To simulate the relative density, the densest sample is packed with an inter-particle friction of zero; conversely, the loosest sample is packed with a friction of 1.0. [5] Compared with Fig. 3, the densest sample shows qualitative agreement; therefore, the following discussion of pore structure adopts this densest packing case. Meanwhile, to focus on a geometric study, the particle diameter and voids are normalized by the minimum particle size.

3.3 Characteristic of pore structure

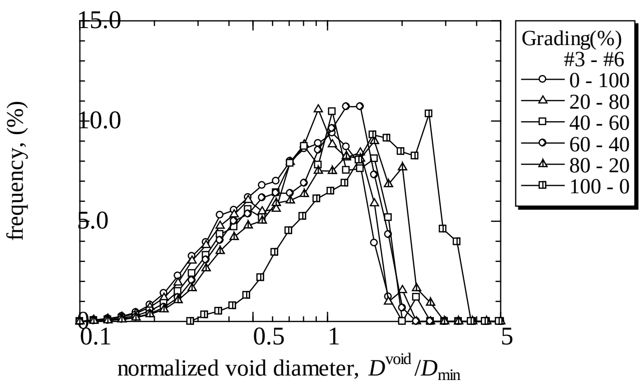

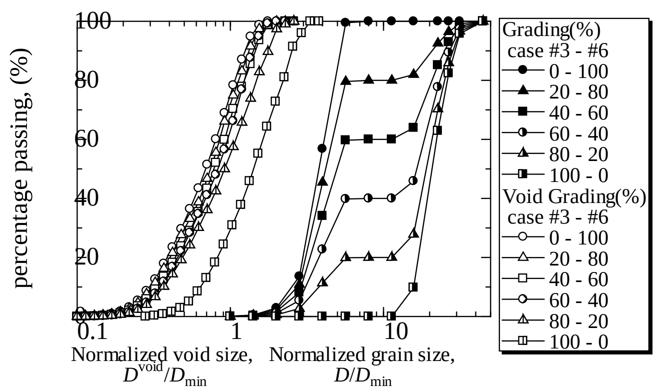

Fig. 11 – Frequency of void size of #3-#6, Fig. 12 – Void size distribution and grain size distribution of #3-#6

Fig. 11 shows the frequency of void size of the #3-#6 mixture case, and Fig. 12 shows this void size distribution with grain size distribution. To make an order from smaller void size frequency, grading series lines along with increasing coarse grain content ratio. Fig. 12 indicates that the void size distribution is almost 1/10 of the grain size distribution and part of the void range has a gap with grading shape. Moreover, Fig. 13 shows the relationship between this normalized void size and the matrix samples of all cases. According to this figure, void size is almost the same in the matrix samples with content ratios greater than 40%.In this content lower than 40%, normalized average void sizes line along with coarse grain size.

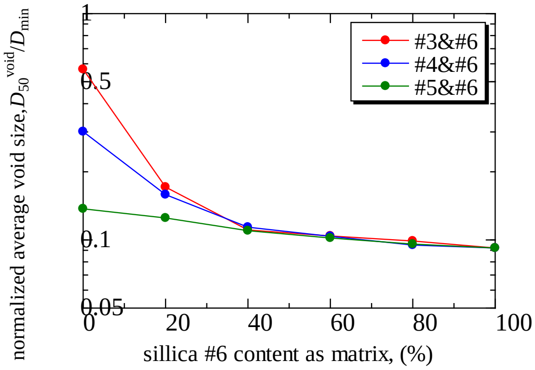

Fig. 13 – Normalized average void size and matrix sand content

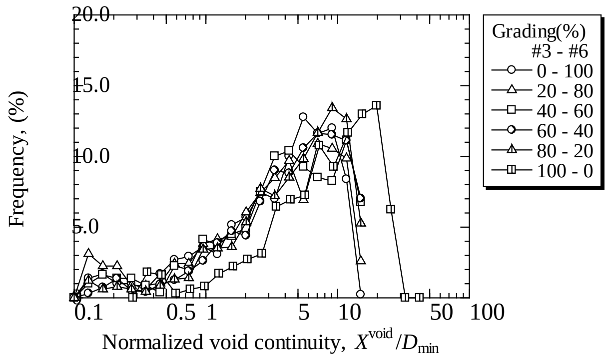

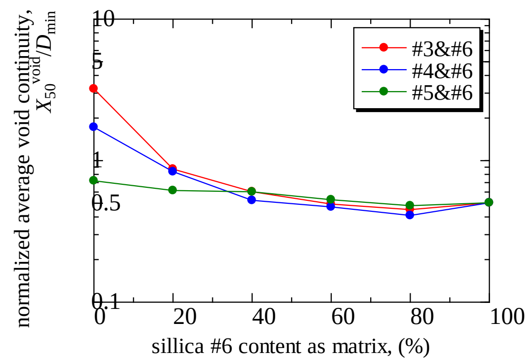

Fig.14 – Frequency of void continuity of #3-#6, Fig.15 – Norm. ave. void continuity and matrix content ratio

Fig. 14 shows the frequency of the normalized void continuity expressed as X^{void} for the #3-#6 mixture case. Fig. 15 shows the relationship between the median of this continuity expressed as X_{50}^{void} and the matrix sample content ratio of all cases. To make an order from higher void continuity, grading series also lines along with increasing coarse grain content ratio. As for Fig. 15, void continuity increases with decreasing matrix sample content below 20%; this content ratio is lower than the void size trend in Fig. 13. This difference arises from that this lower content relates larger void sizes content ratio; this larger void existence leads connection of voids higher. According to this point, Fig. 16 shows the proportional relationship between the normalized average void size and its continuity. In addition, this proportional line has a negative intercept; therefore, void sizes limit the existence of void continuity.

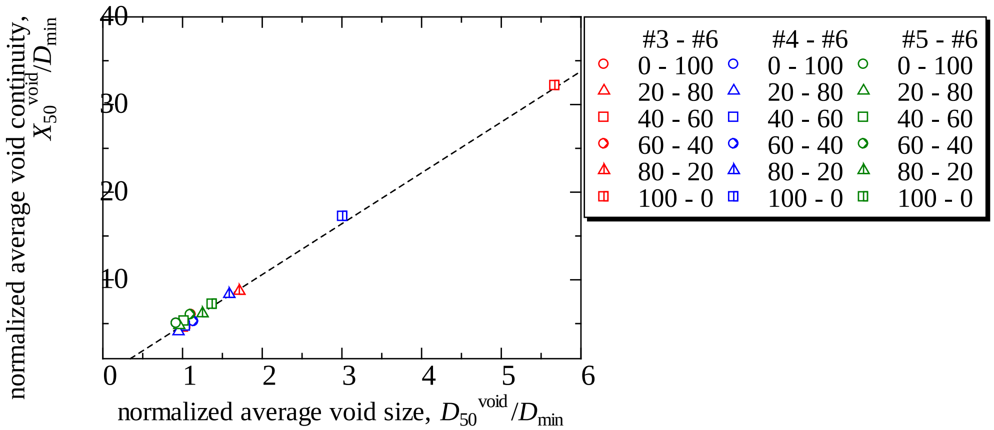

Fig. 16 – Relationship between void size and its continuity in various grading shapes

3.4 Relationship between permeability and pore structure

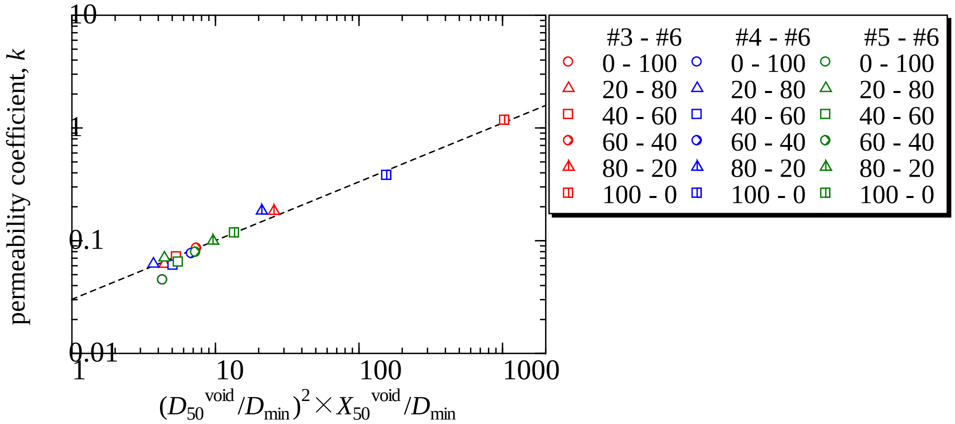

Fig. 17 – Expression of permeability coefficient with pore structure

This section aims to express the relationship between macroscopic permeability and pore structure. Fig. 17 shows this relationship by expressing pore structure by multiples of void size and void continuity expressed as $(D_{50}^{void}/D_{min})^2 \times (X_{50}^{void}/D_{min})$, which refers basis of Taylor formula expression in equation (1): normalized median void size term (D_{50}^{void}/D_{min}) assumes to correspond with the representative grain size term as the hydraulic radius, normalized median void continuity term (X_{50}^{void}/D_{min}) assumes to correspond with the void ratio function term as above mentioned flow channel property. This relationship shows good agreement with that in Fig. 7, which adopts the median grain size as D_{50}.

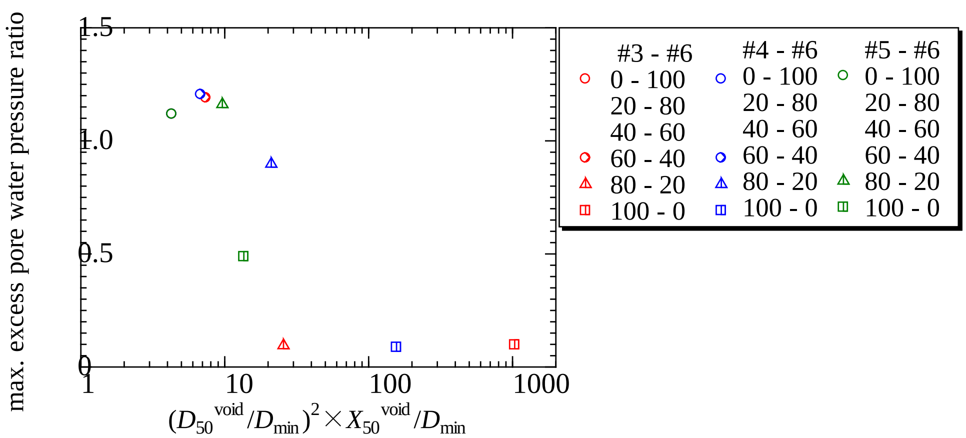

Fig. 18 – Boundary of pore structure for increasing excess pore water pressure

According to the good agreement with permeability, Fig. 18 shows the relationship between this pore structure expression and maximum excess pore water pressure ratio in the experiment. This shows a trend similar to that in Fig. 6. Therefore, pore structure also can be expressed as a boundary for increasing excess pore water pressure.

4. Conclusion

In this study, from the viewpoint of pore structure, the liquefaction potential based on permeability and grading shape is examined. The pore structure mainly consists of void size and its continuity. To find a relationship, we conducted a shaking table test and numerical simulation using a discrete element method adopting binary grading, which consisted of mixed silica sand #3 to #6. In the experimental result, each maximum excess pore water pressure ratio showed agreement with its densest mixture content ratio, which content ratio also proportional to finer content ratio. As for agreement with the experimental result, the pore structure indices expressed by multiples of void size and void length show qualitatively good correspondence with permeability and increasing excess pore water pressure content ratio.

5. References

[1] Numata, A. Mori, S. (2002): Grain size distribution of erupted sands due to liquefaction. *Journal of JSCE*, **722**(61), 129-147.

[2] Iai, S., Koizumi, K., Tsuchida, H. (1986): A new criterion for assessing liquefaction potential using grain size accumulation curve and N-value. *Report of the port and harbor research institute*, **25**(3), 125-234

[3] Yamazaki, H., Zen, K., Koike, F. (1998): Study of the liquefaction based on the grain size distribution and the SPT N-value, Technical note of the port and harbor research institute, **914**, 3-31

[4] Kenny, T.C., Chahal, R., Chiu, E., Ofoegbu, G.I., Omanege, G.N., Ume, C.A. (1985): Controlling construction sizes of granular filters, *Can.Geotech. J.*, **22**. 32-43.

[5] Maeda, K. Kondo A. (2014): Effects of grading shape on internal erosion focusing pore structures and finer dynamics. *Journal of JSCE*, **70**(2), I_507-I_517.

[6] Cundall, P. A., Strack, O .D .L. (1979): A discrete model for granular assemblies. *Geotechnique*, **29**(1), 47-65.